IMPACT: International Journal of Research in Humanities, Arts and Literature (IMPACT: IJRHAL)
ISSN (P): 2347–4564; ISSN (E): 2321–8878
Vol. 7, Issue 3, Mar 2019, 577–590
© Impact Journals

HIGH SPEED 8/6 SWITCH RELUCTANCE MOTOR POWERED BY SOLAR PHOTOVOLTAICS ALONG WITH THE FREQUENCY VARIATION

Neeraj Solanki[1] & Virendra Kumar Sharma[2]

[1]Research Scholar, Department of Electrical Engineering, Bhagwant, University, Ajmer, Ajmer, Rajasthan, India

[2]Professor, Department of Electrical Engineering, Bhagwant, University, Ajmer, Ajmer, Rajasthan, India

Received: 12 Mar 2019 **Accepted:** 19 Mar 2019 **Published:** 31 Mar 2019

ABSTRACT

This paper gives a solar photovoltaic (SPV) array, water pumping machine using a High speed 8/6 switched reluctance motor drive. The virtual commutation of High speed 8/6 switched reluctance motor drive (SRM) power at critical frequency gives decreased switching losses in a mid-factor converter and drastically Increases the efficiency of proposed system. The velocity of High speed 8/6 switched reluctance motor drive (SRM) is controlled by using numerous DC- Bus voltage of the mid-point converter. A DC - DC Boost converter running in continuous conduction mode (CCM) is used for DC-Bus voltage manipulates. The continuous conduction mode (CCM) operation of inductors helps to reduce the ringing impact and decreases the losses of DC-DC converter. Present day and voltage stresses on devices which consist of switching pressure of Boost converter are also reduced in continuous conduction mode (CCM). The Boost converter facilitates the non-stop and clean input/output currents to High speed 8/6 switched reluctance motor drive (SRM) force with boundless place for maximum power point tracking (MPPT) operation. The adjustment in step length of an incremental conductance (InC) maximum power point tracking (MPPT) set of policies helps the smooth starting of High speed 8/6 switched reluctance motor drive (SRM) force. The proposed system, subjected to dynamically atmospheric situations is designed, Modeled and simulated the usage of Matlab / Simulink environment. A prototype of proposed configuration is likewise superior and its performance is established with test results for manipulate of pace over various insolation ranges.

KEYWORDS: *Solar Photovoltaic (SPV), High Speed 8/6 Switched Reluctance Motor Drive (SRM), Continuous Conduction Mode (CCM), Maximum Power Point Tracking (MPPT)*

INTRODUCTION

It`s very easy process to supplying water in sufficient quantities according to requirement, defensive fitness and ensuring sustainable development are important issues for farmers and ranchers, widespread water deliver in a ways flung places is required to make certain with grazing flippantly. Solar Photovoltaic (SPV) array based totally water pumping is maximum widely wide-spread and famous software of Solar Energy in growing countries. Solar Energy primarily based water pumping system is green along with emission reduction of CO2, dependable and value effective for farm animals watering, irrigation purposes and for delivery of water for home applications in far flung places. Different DC and AC automobiles have been proposed thus far in SPV array primarily based water pumping machine. The troubles associated with DC cars are the normal preservation requirement due to presence of commutator and brushes. On The alternative side, AC motors have inability to perform at low speeds, complicated manage and low reliability. SPV powered everlasting magnet vehicles

(PMBLDC / PMSM) for water pumping utility using numerous Maximum power point tracking (MPPT) strategies were studied using diverse intermediate DC - DC converters. DC motor, PMSM and an induction motor are in comparison and concluded that special machines are higher preference for worldwide performance optimization of SPV water pumping system. The disadvantage of brushless DC motor (BDCM) power system is a complex control method and complex inverter topology. The most important disadvantage with these automobiles is the phenomenon called irreversible demagnetization of everlasting magnets among all unique machines, 8/6 High Speed Switched Reluctance Motor (SRM) has the simplest production. The rotor of SRM includes no conductors or permanent magnet. Because of its immoderate torque density, low inertia, quick reaction, variable losses and large velocity variety functionality, SRM can be suitable to candidates for water pumping which shall be powered through SPV. The stator windings of SRM are electrically separated, for this reason, the selection of converter topology and control approach has more flexibility than some different force system, each t SRM and permanent magnet (PM) machines are free of rotor copper loss however the SRM levels are independently managed via the converter.

Which make the fast circuit cutting-edge decay quickly even as inside the PM machines quick circuit contemporary persists, long as the system continues to rotate due to lower back - emf generation. The sturdy brushless creation and right thermal functions make the SRM force appealing for SPV powered water pumping device. Many topologies of SRM pressure water pumping machine had been mentioned inside the literature but every suffer from some dangers like absence of MPPT tracker, requiring large range of sensors, gadget complexity due to use of battery and many others.

Figure 1 indicates a traditional scheme of SPV increase converter based water pumping gadget making use of SRM force. It Includes a SPV array, a lift converter, a battery with a bidirectional converter and a 3 segment SRM together with its power circuit and water pump it really is proposed. This type of scheme has its personal drawbacks like bargain in performance and reliability due to the working voltage of complete machine that is absolutely regulated by means of the usage of the battery despite SPV array and further losses because of bidirectional converter. The opposite obstacles of this machine are absence of MPPT operation, high SRM inverter losses because of PWM switching and its complexity. The switching losses are minimized by the use of a concept of variable dc-link voltage for velocity manages of motor pressure.

Proposed System

Figure 2 shows the proposed SPV array water pumping system using a Boost converter and employing SRM pressure. It includes the SPV array, a Boost converter, the mid-factor converter feeding, the SRM and a coupled water pump. The Boost converter is so designed and its parameters are decided directly to function in CCM mode. The CCM operation of Boost converter allows to reduce the modern and voltage stresses on its devices and to understand the DC - DC conversion ratio unbiased of load.

The troubles found in Discontinuous Conduction Mode (DCM) like ringing phenomenon that is due to the transition of voltage at the alternative forestall of the inductor while the pulses for fundamental switching of The midpoint converter switches are generated from The corridor impact function sensors located on the stator part of SRM and its helps to reduce The loss associated with switches of a mid-point converter. The SPV array output electricity is optimized by means of (InC) Maximum Power Point tracking (MPPT) approach. The layout and control of the proposed system are elaborated inside the following sections. A prototype of proposed configuration is also developed to validate its overall

performance for varying insolation degrees. The experimental consequences are used to validate the worthiness of proposed system.

Proposed SPV water pumping system operation with the of DC – DC boost converter, MPPT used for maximum power pint tracking to track the maximum power to operate the SRM, Variable Frequency Driver (VFD) is important to control the electricity variation control, to operate SRM with high reliability.

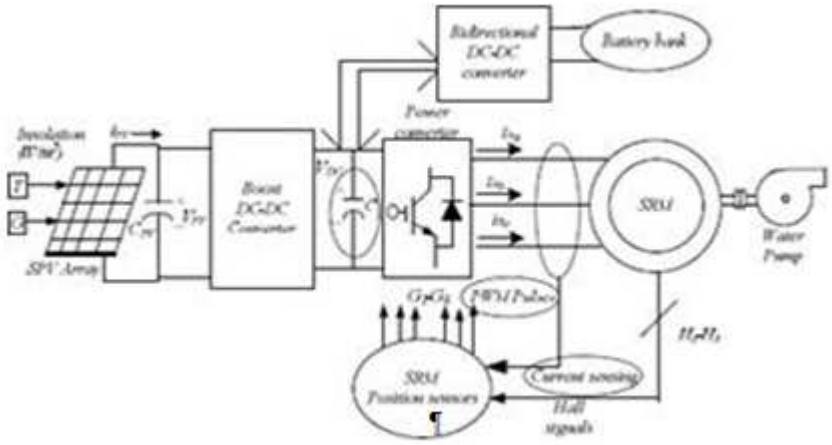

Figure 1. Conventional SPV, SRM Driven Water Pumping System.

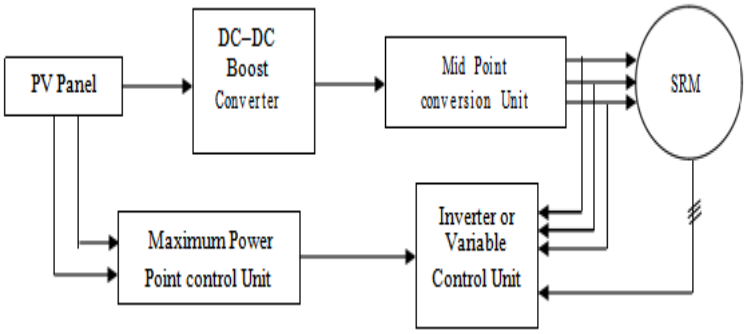

Figure 2. Proposed SPV Powered SRM Driven Solar Water Pumping System Utilizing Boost Converter

Design and Modelling of Proposed System

Since the PV technology power amount not to be stable due to the reason of current variation at every movement instant of time but voltage not to be changed at the every movement instant of time according to power low, power will be varied every instant of movement in the form of micro second so we are going to equate and evaluate the weather movement over the day because, I am looking weather condition to increased the SRM performance and reliability over the day important parameter of PV modules rated and rating effects on the PV module over the time and day

Design and Modelling of SPV Array

A SPV array of 900 W top electricity capabilities, incredibly higher than SRM pressure rating (750 W) is selected so via thinking about some losses are usually associated with converters and the motor. All the parameters of SPV array are predicted at 1000 W/m^2 insolation level. A solar PV module has short circuit module cutting-edge (I) of three.55

and open circuit module voltage (Vocn) of 21 V every SPV module has a potential of 50 W. The electric specs of hb-12100 and designed SPV array at 1000 W/m^2 are envisioned in table I. consequently, an array of 900w peak electricity capability is designed with 1 module in parallel and 17 modules in collection with a PV array of 1*17 modules.

PV modules are rated in terms of their **Peak Power** (**Wp**) output under standard test conditions (STC) **STC** condition refers to

- Irradiation: 1000 W/m^2,
- AM1.5G global solar radiation
- Cell or module temperature: 25^{o}C
- Wind speed: 1 m/s.
- **SOC** (Standard Operating Conditions) - for more realistic figure for the possible power output from a PV module **NOC** (Nominal Operating Conditions)
- Irradiation: 800 W/m^2,
- Ambient temperature: 20^{o}C

Nominal Operating Cell Temperature (NOCT)

The temperature reached by a cell in open circuited module under (**NOC)** conditions used to give more realistic cell temperature of the module under operating conditions. The (**NOCT)** lies usually between **42** to **50^{o}C Module**

Temperature (Tmod)

Where **Tamb** - ambient temperature, **P**in is the solar irradiation in **kW/m^2 I-V c**urve of a module change with illumination case study over the day or month or year

Figure 4 shows the power output increase as the module voltage increases it reaches to a peak (called the Peak Power) and it drops as the voltage approaches to the open circuit voltage

Calculate the output power from a solar cell if its efficiency is 21, 19, 17 and 15 %, input power density is 1000 W/m^2 and area of solar cell is 100 cm^2. Current produced by a PV module is linear function of the radiation intensity the power of a module decreases almost linearly with the decrease in intensity of solar radiation Solar irradiation available throughout the day is varying Voltage of a module is logarithmic function of the radiation intensity, almost constant. Power output changes as radiation changes.

I-V curves and power variation of a 75 Wp solar PV module at 25^{o}C as a function of variation in solar radiation intensity. Dotted line shows the maximum power point line.

The output power of a solar PV modules also depends on the temperature at which module is operating the current increase with temperature due to decrease in the band gap of Si, the increased cell temperature results decrease in the open circuit voltage due to increase in reverse saturation current. Peak power decreases with increase in module temperature.

The maximum rated power point of a crystalline silicon solar cell is 2.5 Wp. Calculate the maximum power output at 45 ^{o}C, 55 ^{o}C, and 65^{o}C cell operating temperature, for crystalline silicon cell decrease in maximum power per degree centigrade increase in cell temperature, (from STC value of 25^{o}C), is 0.45%/^{o}C. Fill the sheet below.

$$T_{mod} T_{amb} \qquad \frac{NOCT20}{0.8} * P_{in}$$

Figure 3

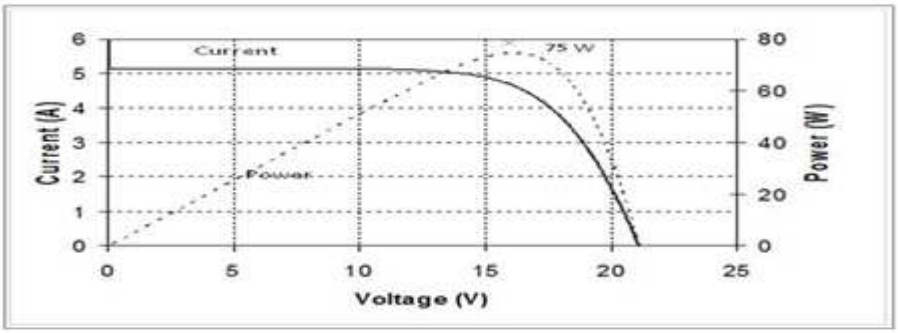

Figure 4

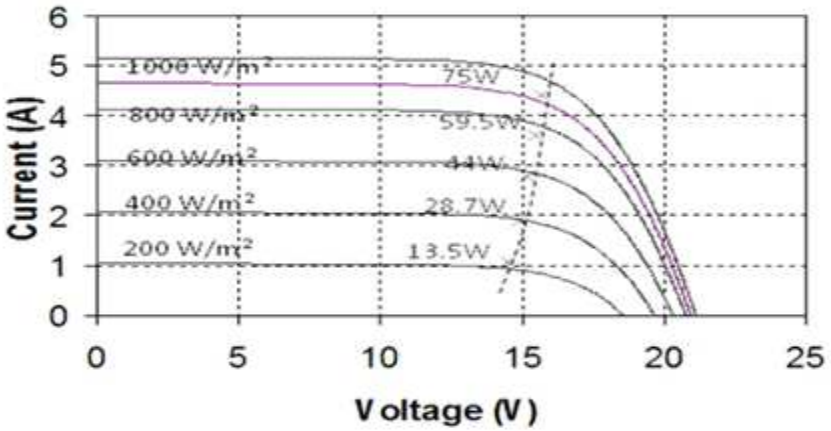

Figure 5

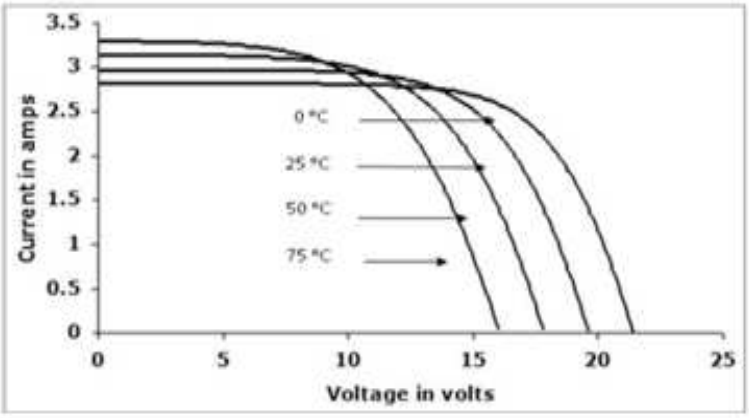

Figure 6

Table 1

Operating Cell Temp. (^{O}c)	STC Cell Temp. (^{O}c)	Different In Temp. T (^{O}c)	Pmax At STC (Watt)	% Decrease In Power Per ^{O}c Rise In Temp.	Decrease In Cell Power At Operating Temp. (Watt)	Actual Maximum Power Point At Cell Operating Temp. (Watt)
A	B	C	D	E	F=E*D*C	G =D-F
45	25	20	---	-0.45%	---	2.27
55	---	---	2.5	---	0.337	---
65	---	---	---	-0.45%	---	---

Design and Modelling of Boost Converter

The DC - DC Boost converter is designed in the sort of way that it usually operates in CCM irrespective of the environmental conditions. The peak and RMS currents are extensively decrease in CCM resulting in decrease losses inside the conduction paths and smaller ringing because the strength stored in inductances is proportional to square of the modern - day. The rated DC voltage of The SRM is as, VDC = 320 V and the PV voltage at MPP is as, VPV = VMPP = 289 V. The relationship between the duty ratio, D of insulated gate bipolar transistor (IGBT) transfer, output voltage, VDC and input voltage, VPV of the boost converter is given. The estimation of the parameters of Boost converter is summarized in table II. The responsibility ratio, D of the boost converter is predicted as

$$DC/PV=/-1=> =VDC/(DC+PV)=320/320+289=0.52\ (1)$$

1= 2= (30−∝)/2 DC

(2)

Wherein, I = DC hyperlink contemporary, = rated angular pace of SRM, = conduction attitude, _VDC = quantity of authorized ripple within the voltage across DC link capacitors C1& C2 i.e. 1.five % of VDC. thinking about pin as W, VDC as 320 V, f as 50 hz and _VC1= _VC2 as 1.five% of VC1,C2,The acquired value of „i" is two.34 a and the received price of C1 = C2 is approx 2441 µf, consequently, C1 and C2 are selected as 2500 µf.

DESIGN AND MODELING OF SRM

The SRM is a doubly-salient reluctance machine with independent phase windings on the stator. The rotor is made of laminations and does not contain any magnets or windings. Different structures of SRM exist based on the number of phases and the number of rotor and stator poles. The basic four phase SRM has eight stator poles and six rotor poles and is named the 8/6 machine due to the pole configuration as shown in figure 3.1(a) & (b). For a four phase 8/6 SRM, the two repetitions of this structure, it becomes a 16/12 machine. Other configurations are possible including 6/4, 4/2, 6/2, 10/4, and 12/10. The fundamental equation relating the machine speed *rpm*, the number of rotor poles *Nr* and the fundamental switching frequency of one phase *f* is given by:

$$f = \frac{rpm}{60} N_r \qquad \text{Hz}$$

(1)

The stator pole, phases and their windings are connected in series and parallel, the combination of series /parallel connections. In the series type connection, current in all coils are same and voltage across with each coil, supply voltage divided by the number of coils, with a parallel connection, voltage across the all coils. The same current supply in each coil, divided by the number of coils assumption, all the coils are balanced.

The 8/6 SRM selected for the project work as shown in below figure 4. With their pole orientation in manner with the degree. The stator poles of 8/6 SRM phase have two winding connected in series, so current in the all coils are same and the voltage across each coils are equal to the half of supply voltage.

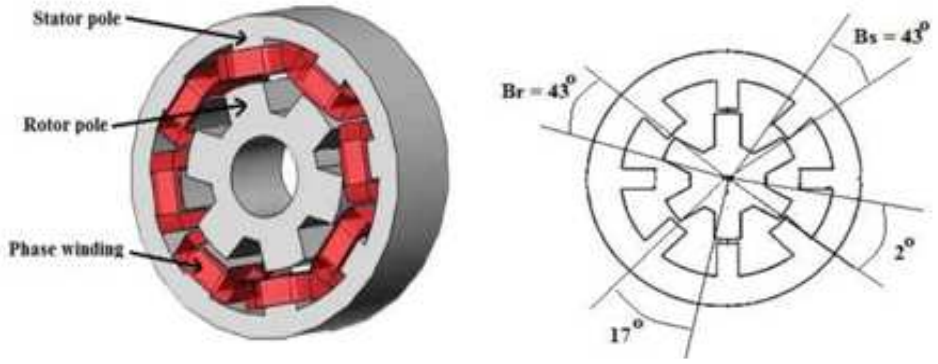

Figure 7: (A) 8/6 SRM Internal Diagram, (B) Stator & Rotor Pole Angles for 8/6 SRM.

The torque production in the switched reluctance motor is explained using the elementary principle of electromechanical energy conversion in a solenoid, as shown in Figure 8 (A). The solenoid has *N* turns, and when it is excited with a current *i*, the coil sets up a flux Φ. Increasing the excitation current will make the armature move towards the yoke, which is fixed. The flux vs. Magneto motive force (MMF) is plotted for two values of air gap, *x*1 and here *x*1 > *x*2, that is shown in figure 8 (B) The flux vs. MMF characteristics for *x*1 is linear because the reluctance of air gap is dominant, making the flux smaller in the magnetic circuit. The electrical input energy is written as.

$$W_e = \int ei\,dt = \int i\frac{dN}{dt} = \int Ni\,d\Phi = \int F\,d\Phi \qquad (2)$$

Where *e* is the induced EMF and *F* is the MMF. This input electrical energy, *We* is equal to the sum of energy stored in the coil, *Wf* and energy converted into mechanical work, *Wm* It is written as.

$$W_e = W_f + W_m \qquad (3)$$

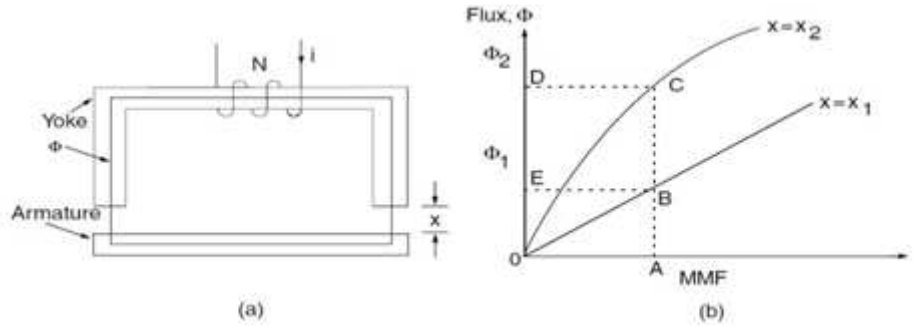

Figure 8: (A) Solenoid, (B) Flux vs. MMF Characteristics.

When no mechanical work is done, as in the case of the armature starting from position *x*1, the stored field energy is equal to the input electrical energy given by equation 8 (A). This corresponds to area OBEO in figure 8 (B). The complement of the field energy, termed co energy, is given by area OBAO in Figure 8 (B) and mathematically expressed

as $\int \Phi dF$. Similarly, for the position $x2$ of the armature, the field energy corresponds to area OCDO and the co energy is given by area OCAO. For incremental changes, equation (3) is written as

$$\delta W_c = \delta W_f + \delta W_m \tag{4}$$

For a constant excitation of $F1$ given by the operating point A in figure 2 (b), the various energies are derived as

$$\delta W_c = \int_{1}^{2} F_1 \, d = F_1(\ 2 - 1\ ) = \text{area(BCDEB)} \tag{5}$$

$$\delta W_c = W_{f|\ x\ x2} - W_{f|\ x\ x1} = \text{area(OCDO)} - \text{area(OBEO)} \tag{6}$$

Using equation (4) to (6), the incremental mechanical energy is derived as

$$\delta W_m = \delta W_c - \delta W_f = \text{area(OBEO)} \tag{7}$$

And that is the area between the two curves for a given magneto motive force. In the case of a rotating machine, the incremental mechanical energy in terms of the electromagnetic torque and change in rotor position is written as

$$\delta W_m = T_e \, \delta\theta \tag{8}$$

Where Te is the electromagnetic torque and $\delta\theta$ is the incremental rotor angle. Hence, the electromagnetic torque is given by:

$$T_e = \frac{W_m}{\theta} \tag{9}$$

For the case of constant excitation (i.e., when the MMF is constant), the incremental mechanical work done is equal to the rate of change of co-energy, which is nothing but the complement of the field energy. Hence, the incremental mechanical work done is written as

$$\delta W_m = \delta W'_f \tag{10}$$

Where

$$W'_f = dF = d(Ni) = N\, di = (\theta, i)di = L(\theta, i)\, i\, di \tag{11}$$

Where the L is inductance, Φ is flux linkages; λ is functions of the rotor position and current. It is change the co-energy occurs between two rotor positions, $\theta 1$ and $\theta 2$. Hence, the air gap torque in terms of the co-energy represented as a function of rotor position and current is:

$$T_e = \frac{W_m}{} = \frac{W_f}{} = \frac{W_f \ i,}{} \Big|_{i=\text{constant}} \tag{12}$$

If the inductance is linearly varying with rotor position for a given current, which in general is not the case in practice, then the torque can be derived as:

$$T_e = \frac{dL}{d}\,\frac{i^2}{2} \tag{13}$$

$$\frac{dL}{d} = \frac{L_2 - L_1}{2 - 1}\Big|_{i=\text{constant}} \tag{14}$$

And this differential inductance can be considered to be the torque constant expressed in N.m/A^2. It is important to emphasize at this juncture but that is not a constant and that it varies continuously.

The torque characteristics of SRM are dependent on the relationship between flux linkages and rotor position as a function of current shown below.

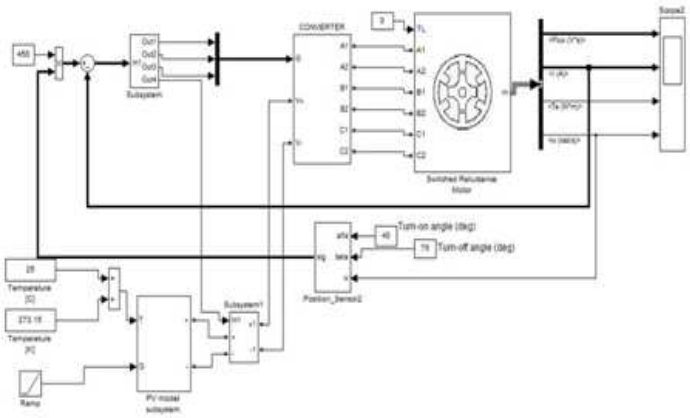

Figure 9: Developed Simulink Model of SRM.

$$T_e = \frac{dL}{d}\,\frac{i^2}{2} \qquad =0.52/$$

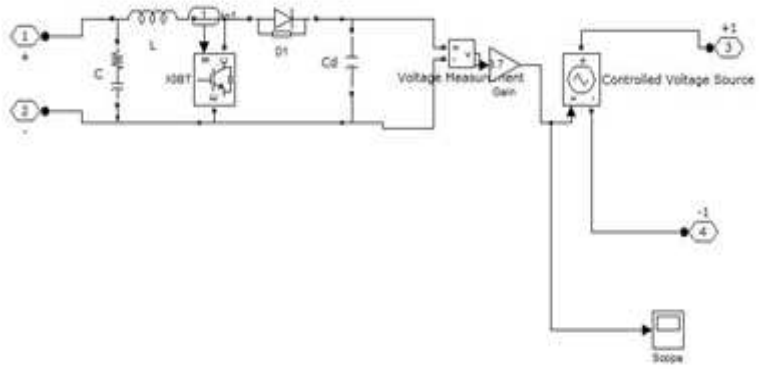

Figure 10: Simulink Model of PV Array (Subsystem).

MPPT Control

The vicinity of MPP in The i-v characteristics of SPV array is not predicted in advance and continually varies dynamically with insolation degrees and environmental situations The governing equations which provide an explanation for The running principle of InC approach areas,

(15)

(16)

In which, *I* & *V* = change in pv modern and voltage in two consecutive samples.

The reference voltage of SPV array is checked for top and decrease limits which are set to 0.7vocmax to 0.9vocmax. incase The Vp Vref is among The boundaries, it is stored as it's far else The VpVref is saturated to The closest restrict. The saturation block output is specific as new reference pv voltage (VpVrefn). The Vp Vrefn and sensed pv voltage are Then used to estimate The duty ratio for The Boost converter. The governing equation for estimating responsibility ratio is,

(17)

Reference duty ratio is compared with saw-tooth waveform to generate switching good judgment for The switch of Boost converter.

Figure 11 (A) suggests a pv curve at The side of all feasible factors on curve undergoing into execution of InC algorithm. Figure 11 (B) explains the method of obligation cycle era via MPPT method and it may be summarizes via all feasible situations for MPPT operations The use of Figure 11 (A).

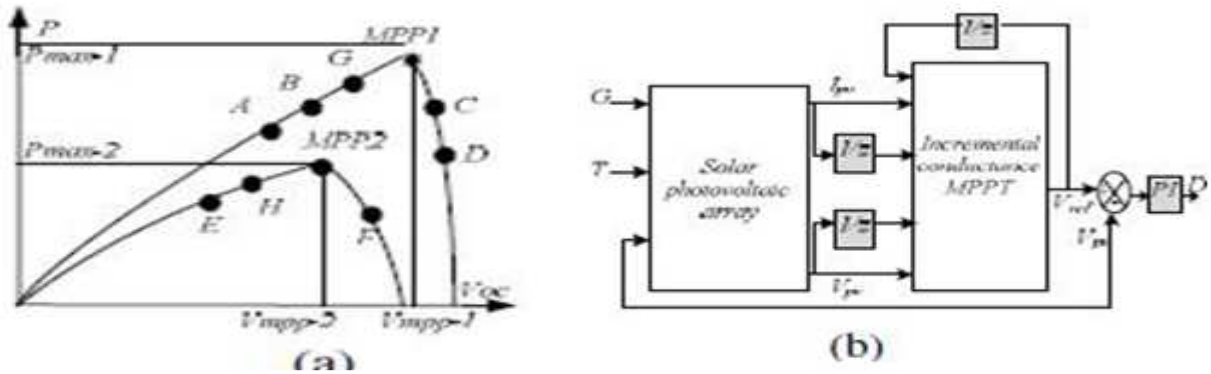

Figure 11: Explanation of Inc Method and Generation of Duty Cycle for DC- DC Converter by Inc Algorithm.

Proportional-Integral (PI) Control

The combination of proportional and integral terms is important to increase the speed of the response and also to eliminate the steady state error. The controller output is given by

(18)

Where is the error or deviation of actual measured value (PV) from the set point (SP). the PI controller eliminates offset error and increases the speed of the response. In this case, the flux and speed from the output is given as input to the PI controller through sum and output of PI controller is given as gate signal to each converter which controls the phases of SRM.

Efficiency Estimation of Proposed System

The efficiency of proposed system at exceptional insolation degrees with motor output strength is given in table I. fig.6 indicates a graphical representation of power and performance with different solar insolation tiers. The proposed system exhibits an efficiency of 83.33% at rated load whilst 75.2% at 600 w/m2.

$S(W/m^2)$	$P_{pv}(W)$	$P_m(W)$	η %
600	555	417.6	75.2
700	647	504	77.9
800	740	590	79.92
900	833	681	82.89
1000	900	750	83.33

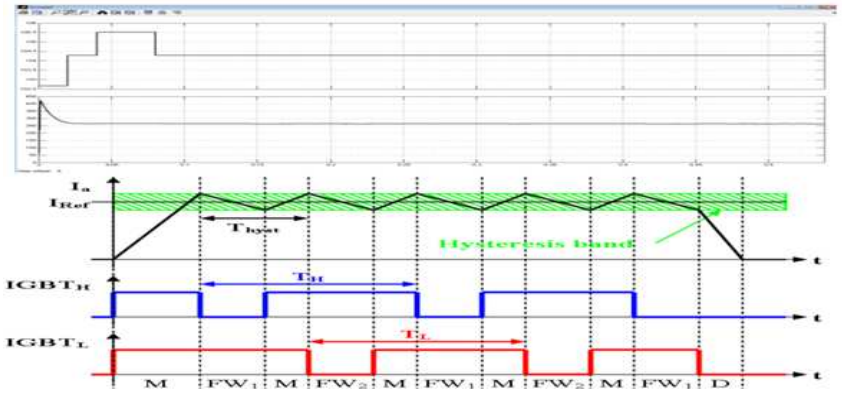

Figure 12: Boost Converter Output.

Parameter Selection for Design of Boost Converter

Switching frequency, *fsw* = 20 kilo Hertz; Input inductor, *Li*= 6.25 milli henry; Output inductor, *Lo*= 6.87 milli henry; Energy transfer capacitor, Cm = 3microFarad, DC link capacitors, C1 = C2 = 2500 micro farad.

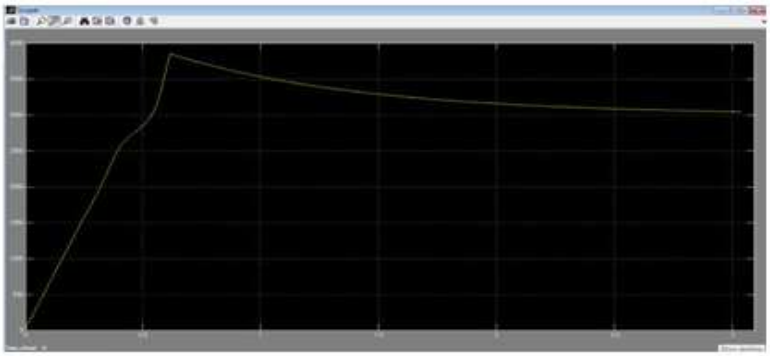

Figure 13: Speed of the Motor in Rotation per Minute.

Switched Reluctance Motor Specification

750W, 8/6 pole, Four phase, 1500 rotation per minute, DC link voltage = 320V.

CONCLUSIONS

The SPV array fed SRM driven water pumping system. The usage of Boost converter has been modeled and its overall performance has been simulated using Matlab/Simulink platform and simulated performance has been tested experimentally using advanced prototype hardware. The overall performance of proposed system has been placed quite properly for various environmental situations. A variable voltage of dc bus has been used for controlling the charge of SRM power which has given freedom for the virtual commutated operation of mid- factor converter which ends up in decreased switching losses of converter. The CCM operation of Boost converter has additionally boosted the overall performance of proposed water pumping gadget through lowering voltage and contemporary stresses on gadgets of Boost converter and growing power output of Boost converter by means of way of reducing the ringing effect of system. The experimental and simulated outcomes have very an awful lot close which has confirmed the version of the proposed SPV fed water pumping the usage of SRM power.

REFERENCES

1. *B. Subudhi, and R. Pradhan, "A Comparative examine on most strength point tracking strategies for photovoltaic electricity systems," ieee transactions on sustainable electricity, vol.4, no.1, pp.89-ninety eight, jan. 2013.*
2. *M.A.G. De Brito, L. Galotto, L.P.Sampaio, G.E Melo De Azevedo and C.A. Canesin, "Assessment of the main MPPT strategies for photovoltaic packages," ieee transactions on business electronics, vol.60, no.3, pp.1156-1167, march 2013.*
3. *Ministry of new and renewable electricity, government of India.*
4. *(2013, might also). World Solarphotovoltaic"s installations, 2000-2012 [Online]. available: https://www.earth-policy.org/data_center/c23*
5. *Ahmed m. Kassem, "MPPT manage design and overall performance enhancements of a pv generator powered dc motor-pump systembased on synThetic neural networks," int. magazine of electrical electricity & electricity structures, vol. forty three, pp. 90-98, december 2012.*
6. *S. G. Malla, C. N. Bhende, and S. Mishra, "Photovoltaic based water pumping system," int. conf. power, automation signal (iceas), 28-30 dec. 2011, pp. 1-4.*
7. *S.Jain, A.Okay.Thopukara, R. Karampuri, and V.T. Somasekhar, "A single- degree photovoltaic systemfor a dual-inverter-fed open-cease winding induction motor pressure for pumping applications," ieee transactions on energy electronics,, vol.30, no.9, pp.4809-4818, sept. 2015.*
8. *B.N. Singh, B. Singh, B. P. Singh, A. Chandra and Okay. Al-Haddad, "Optimized overall performance of Solar powered variable velocity induction motor pressure," court cases of The 1996 worldwide conference on strength electronics, drives and electricity structures for business growth, 1996, vol. no.,1,eight-11jan1996, pp.58-66.*
9. *G.J.Kish, J.J. Lee and P.W. Lehn, "Modelling and control of photovoltaic panels using The InCremental conductance technique for optimum energy factor monitoring," iet renewable electricity technology, vol.6, no.four, pp.259- 266, july 2012.*

10. *D.Sera, l. maThe, T.Kerekes, S.V. Spataru and R.Teodorescu, "At the perturb-and-examine and In Cremental conductance MPPT strategies for pv structures," ieee journal of photovoltaics, vol.3, no.3, pp.1070-1078, july 2013.*
11. *Mohamed M. Algazar, Hamdy Al-Monier, Hamdy Abd El-Halim and Mohamed Ezzat el kotb salem, "most electricity point tracking The usage of fuzzy common sense control," international journal of electrical electricity & electricity structures, vol. 39, no. 1, pp. 21-28, july 2012.*